



Research and Development of Vibration Control Device for Aerogenerator Using Elasto-Plastic Restoring Force Characteristic

O. Furuya⁽¹⁾, H. Kurabayashi⁽²⁾ and S. Cho⁽³⁾

⁽¹⁾ Associate Professor, Tokyo Denki University, osamu.furuya@mail.dendai.ac.jp

⁽²⁾ President, Vibro-System., h-kura@os.rim.or.jp

⁽³⁾ President, INNOSE TECH Co.,LTD., sgcho@innose.co.kr

Abstract

Aerogenerators have been used in various countries recently as a power generation system to produce environmentally friendly energy. Many countries have been promoting their national projects to examine the construction of the wind-turbine power-generating stations in the ocean. In general, the structure of an aerogenerator is heavy at the top due to the higher position of the center of gravity as a heavy nacelle is set at the top of the aerogenerator tower. Because the dynamic response of an aerogenerator increases greatly due to the top position of the heavy weight, reductions in the responses and improvements of the seismic and wind resistance levels are necessary. This study examined a response control system which is designed to reduce the structural responses and to upgrade the resistance performances against earthquakes and wind excitation. In this paper, a design method and loading tests of elasto-plastic dampers are introduced to investigate the mechanical characteristics of them. In order to confirm the structural seismic and wind response control effects by the damping devices, preliminary analyses and a set of vibration tests using a 1/16-scale model of an aerogenerator were conducted. The results obtained from analyses and tests are reviewed.

Keywords: Aerogenerator, Vibration control device, Elasto-Plastic damper, Loading test, Time response analysis

1. Introduction

At present, Japan has entered a high seismicity recurrence period. Therefore, it is necessary to improve the seismic safety design to upgrade the seismic resistance capabilities of various structures. Moreover, instances of damage caused by strong winds such as typhoons and tornados have increased in the recent years. Under these circumstances, the installation of aerogenerator to provide an uninterrupted supply of electricity has become more attractive in order to reduce greenhouse gas emissions. Recently, building the aerogenerator in the ocean has been considered as a potential national project in Japan. Meanwhile, the risks of damage to aerogenerators [1] caused by strong winds and earthquakes are assumed to have increased with the increasing number of aerogenerators.

Damage to aerogenerators can be divided into two categories [2,3]. The first is damage to the long rotor blades in the nacelle, which is the heaviest part of the aerogenerator, and the second is damage to the support structure, including the underground pedestal. In general, a heavy electric generator, which operates the rotor blade, is set at the top of the aerogenerator. The structural response greatly increases therefore due to the higher center of gravity of the aerogenerator. The aerogenerator now requires to reduce the dynamic responses and to improve the structural resistance capacity levels against earthquakes and winds.

One of the ways to solve such problems is to develop an enhanced damping device that is capable of controlling the dynamic response of the structure. While the damping element consumes vibration energy to transfer it into

heat, the heat caused by damping has an effect not only on the nonlinearity of the temperature-dependency but also on the deterioration of the damping performance. The damping performance against cyclic loading with a large deformation will be important especially under seismic and wind input motions with long durations. In addition, a systematic cost reduction for manufacturing the damper used in large-scale structures represents another important task to extend the application of such a component to more structures. An elasto-plastic damper made of a metal material can be regarded as an effective vibration controller to meet the design requirements. However, it is expected that an elasto-plastic steel damper would be greatly deformed under seismic force. Furthermore, even when a steel damper is subjected to low-magnitude motion, a cumulative fatigue problem may arise due to the repeated deformation of the damper over the long term. This possibility was confirmed in the previous experimental studies of piping systems [4,5].

The present study examines a response control system using an elasto-plastic damper [6-10] which was developed to reduce the dynamic responses of an aerogenerator and to upgrade its resistance performance against earthquakes and wind excitation. For the purpose, a steel damper in the shape of coil spring was designed to develop uniform stress on the whole body when the metal material is under dynamic loading and to obtain the reduction of the low cycle fatigue under large deformation in an effort to improve the repetitive strength during an earthquake with long duration. Moreover, the cyclic strength should be strong enough to withstand vibration induced by wind, especially a large typhoon. By using the metal material known as SS400, which is one of the most commonly used hot rolled general types of structural steel, the manufacturing cost of the damper can be effectively reduced. This paper includes discussions on the design method of an elasto-plastic damping device, a loading test to investigate the mechanical characteristics of the damper, an examination of an analytical model and the preliminary analysis to confirm the response control capabilities against the seismic and wind motions, and a vibration test using a 1/16-scale model with dynamic characteristics.

2. Elasto-Plastic Coil Spring Damper

The damping effect of an elasto-plastic coil spring damper(CSD) is very high not only because the stress of coil is uniformly distributed without stress concentration but also because the entire coil spring can be used as a damping element to utilize the hysteresis characteristics of metal material. As a result, the fatigue characteristics of the damper were dramatically improved and the economic life cycle became longer. Consider the general shape of a coil spring to be developed for the design formulas of the CSD with dimension as shown in Figure 1.

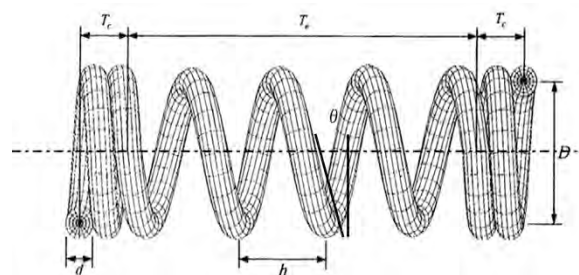


Figure 1 Dimension of elasto-plastic coil spring damper

Where, the symbols indicate:

d : wire diameter

N_e : effective number of turns

D : coil center diameter ($= 2R$)

h : pitch

T_e : effective deformation part ($= hN_e$)

T_c : coherent part

T_e : seat winding part

G : shear modulus of steel

δ_y : yield deformation

F_y : yield force of coil spring damper

f_{sy} : yield stress

k_e : elastic spring constant

k_p : plastic spring constant

E_{s1} : elastic modulus of steel in elastic range

E_{s2} : elastic modulus of steel in plastic range

The prediction formula for the hysteresis dynamic behavior of an elasto-plastic CSD was set up from a parametric study as follows. By using these equations, the mechanical characteristics of CSD is designed.

$$\delta_y = 1.91 \frac{f_{sy}}{E_{s1}} \pi D N_e \left(\frac{D}{d} \right) \quad (1)$$

$$F_y = 0.36 f_{sy} \frac{\pi d^2}{4} \left(\frac{D}{d} \right)^{-1} \quad (2)$$

$$k_e = 0.19 \frac{\pi d^2}{4} \frac{1}{\pi D N_e} \left(\frac{D}{d} \right)^{-2} \quad (3)$$

$$k_p = 0.024 \left[E_{s1} \frac{\pi d^2}{4} \frac{1}{\pi D N_e} \right] \left(\frac{D}{d} \right)^{-1.28} \left(\frac{h}{D} \right)^{0.22} \left(\frac{E_{s1}}{E_{s2}} \right)^{-0.75} \quad (4)$$

3. Experiment on the Elasto-Plastic CSD

3.1 Experimental Specimen

A set of loading tests was conducted to evaluate the mechanical characteristics of the CSD. Five different specimens were designed and manufactured for the study. Table 2 shows the design specifications and the shapes of the test specimens.

Type (A) is the basic type of CSD, using SS400 in the form of a wire rod. Type (A+B) was manufactured to investigate the restoring performance against residual displacement, with a coil spring installed into the CSD. Type (A+C) was constructed by combining the CSD with a viscoelastic damper. This type was used to examine the extent to which the damping capacity was improved in the response control damper in the small deformation region under the yield displacement of the CSD. Types (D) and (E) were manufactured to compare the hysteresis damping characteristics of SS400 and SWRM, which are commonly used as materials of elasto-plastic damping.

3.2 Experimental Method

Table 2 shows the loading test items. The loading test was conducted to investigate the displacement and frequency dependency on the mechanical characteristics. The loading frequency ranged from 0.05Hz to 0.5Hz according to the maximum velocity performance of the loading apparatus. The fundamental loading frequency was 0.3Hz. The displacement amplitude of loading ranged from 2mm to 80mm. Figure 3 shows the loading test conditions as established for the hydraulic servo-actuator. The displacement transducer and load cell installed in the hydraulic servo actuator system were used to measure the displacement and the force. The sampling frequency was set to 50 Hz and to 100 Hz. In addition, the temperatures on the surface of the damper specimens were measured before and after the loading test using a contact-type thermometer.

Table 1 Experimental specimens used for the loading test


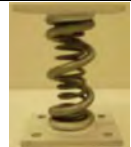



Element	(A)	(B)	(C)	(D)	(E)
Wire rod	SS400	SUP	Material: Urethane elastomer Hardness: 20 ° Outer diameter: 48.6mm Inner diameter: 31.8mm Length: 100mm	SS400	SWRM
Wire diameter [mm]	16	8		6	6
Center diameter [mm]	76	50		43	43
Effective number of turns	3	8.5		5	5
Total number of coils	6	15.5		8	8
Free length [mm]	220	220		234	234
Primary rigidity [kN/m]	491	37.9		32.0	32.0
Secondary rigidity [kN/m]	19.6	-		1.28	1.28
Yield displacement [mm]	6	-		10	10
Yield load [kN]	2.94	-		0.320	0.320
Bilinear factor	1/25	-		1/25	1/25
Maximum displacement	100	80		60	60
Maximum load [kN]	4.79	3.03		0.384	0.384
Test Specimen Type	CSD (A)	CSD (A+B)		CSD (A+C)	CSD (D)
					

Table 2 Loading frequency and amplitude used for the test

		Loading Amplitude [mm]														
		2	4	5	6	8	10	12	15	20	30	40	50	60	70	80
Loading frequency [Hz]	0.05															
	0.3															
	0.5															

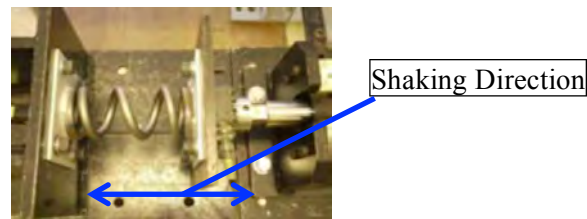


Figure 2 Experimental set-up of loading test

3.3 Experimental Results

Figure 3 shows a comparison of the hysteresis characteristics using different types of wire rods on CSD types D and E. It was confirmed that CSD type D, using the SS400 wire rod, has restoring force characteristics very similar to those of CSD type E, which uses a type of steel with a low yield strength steel level, widely used to fabricate elasto-plastic dampers. Therefore, the damper using SS400 as the elasto-plastic material would deliver good and effective damping performance while also reducing the cost.

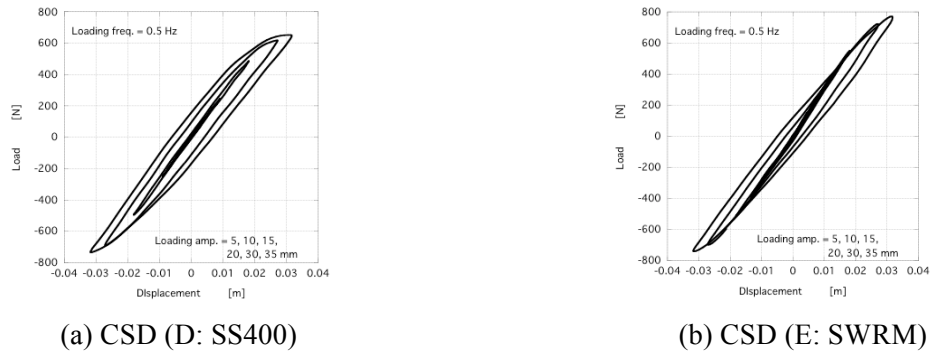


Figure 3 Comparison of hysteresis characteristics using different types of wire rod on CSD (D) and CSD (E)

Figure 4 shows the results of the comparison of the damping performance capabilities over a large deformation area for CSD types A and A+B. For damper type A+B, the spring constant was increased due to the addition of an elastic coil spring to the damper type A. However, it was confirmed that both cases show stable elasto-plastic damping characteristics, even over a region with considerable deformation.

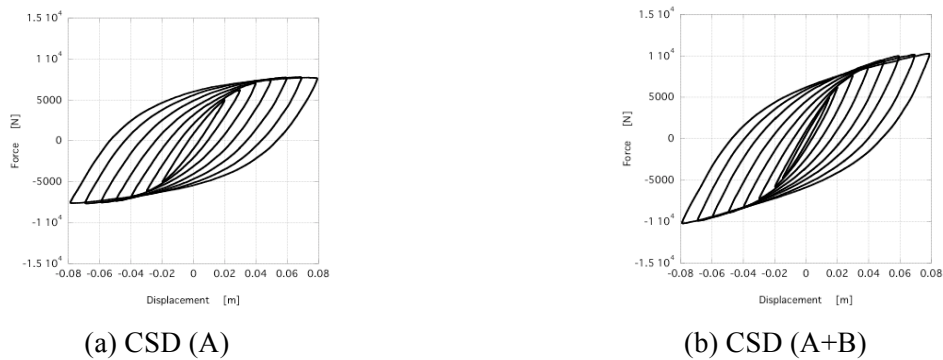


Figure 4 Comparison of damping performance in large deformation area using CSD(A) and CSD(A+B)

Figure 5 shows the characteristics of CSD types A and type A+C over a small displacement region. Damper type A+C readily absorbs energy by larger hysteresis damping in the region of small deformation due to the addition of a viscoelastic damper in damper A. The damping is typically small for elasto-plastic damper (damper type A) prior to yielding of it. Figure 6 shows the results of a comparison of the mechanical characteristics with regard to displacement-dependency using CSD types A, A+B, and A+C. It was confirmed that each damper has specific mechanical characteristics suitable for the damper design as proposed here.

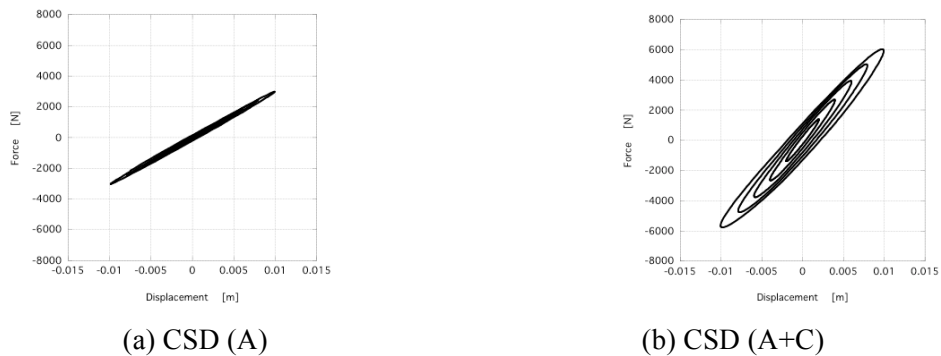


Figure 5 Comparison of damping performance in small deformation area using CSD(A)

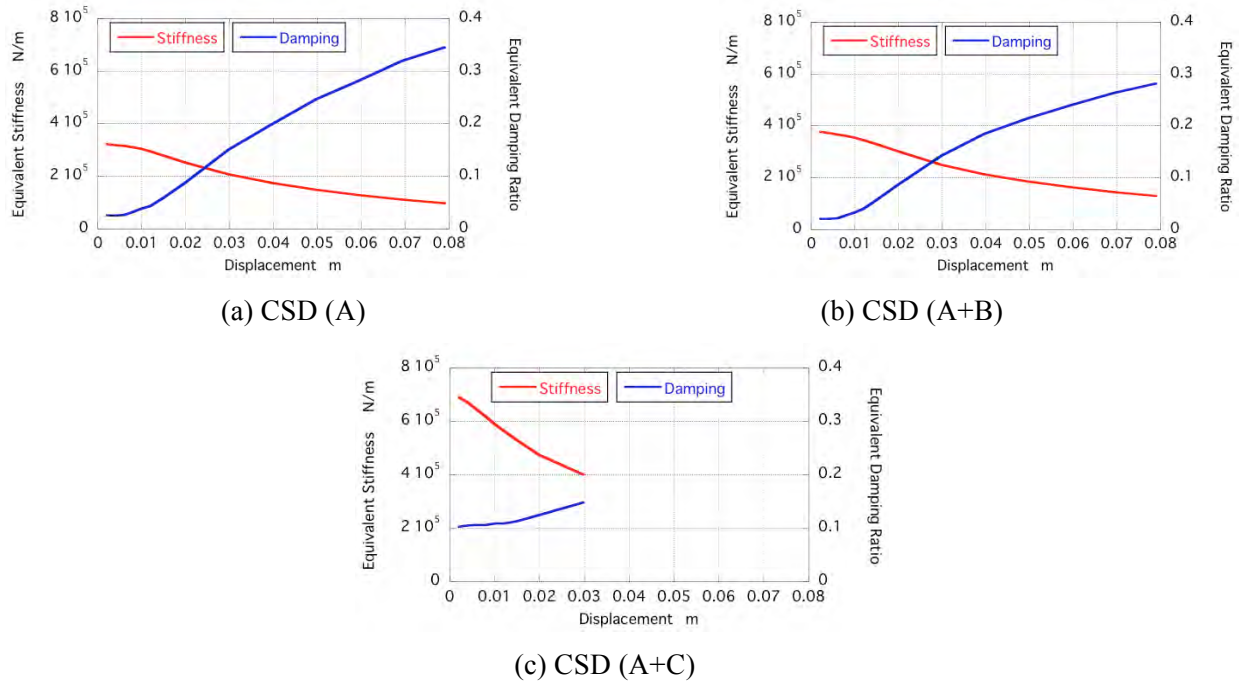


Figure 6 Comparison of mechanical characteristics in displacement dependency using CSD(A), CSD(A+B) and CSD(A+C)

4. Examination of Analytical Model

Based on the results obtained from the loading test, the analytical model was developed to evaluate the damping performance in a time history analysis. The Rate Model [11] was selected to express the damping force characteristic. The formulation of the Rate Model is shown by formulas (5) through (8).

$$\dot{F} = k_1 \dot{X} \left\{ 1 - \text{sgn}(\dot{X}) \left(\frac{F}{F_y} - S \right)^n \right\} \quad (5)$$

$$S = \frac{k_2}{F_y / X_y - k_2} \left(\frac{x}{X_y} - \frac{F}{F_y} \right) \quad (6)$$

$$F_y = k_1 X_y \quad (7)$$

$$k_2 = \gamma k_1 \quad (8)$$

where,

- F restoring force of coil spring damper
- S correction coefficient
- n correction coefficient for shape of hysteresis loop
- X displacement of coil spring damper
- X_y yield displacement of coil spring damper
- F_y yield force of coil spring damper
- k_1 spring constant in elastic deformation
- k_2 spring constant in plastic deformation
- γ bilinear coefficient

Figure 7 indicates the comparison of analytical and experimental hysteresis loops in the case of CSD type A. Loading frequency of 0.3Hz and loading displacement amplitude of 80mm were applied as the experimental conditions. As shown in Figure 9, the analytical results are very coincident with the experimental results.

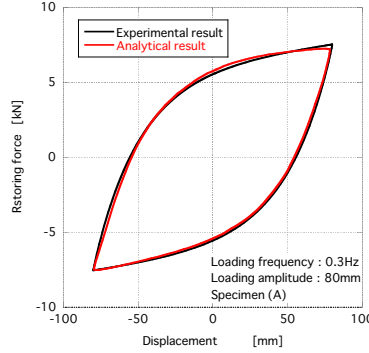


Figure 7 Comparison of analytical and experimental hysteresis loops

5. Preliminary Analysis for Investigation of Vibration Control Effect

The vibration control effect was evaluated by the time history response analysis using the analytical models of response control devices. Two different types of response control devices were examined: Tuned mass damper (TMD) and elasto-plastic CSD. TMD has been examined as a typical type of vibration control device for standard aerogenerators. In this study, TMD was set to be optimal condition of damping and tuning.

The aerogenerator was modeled as a single degree of freedom model based on that the natural frequency of the first mode dominates in the analytical model. The equation of motion of TMD is shown as follows:

$$\left. \begin{aligned} m_s \ddot{x}_s + c_s \dot{x}_s + k_s x_s - c_d (\dot{x}_d - \dot{x}_s) - k_d (x_d - x_s) &= -m_s \ddot{z}_H \\ m_d \ddot{x}_d + c_d (\dot{x}_d - \dot{x}_s) + k_d (x_d - x_s) &= -m_d \ddot{z}_H \end{aligned} \right\} \quad (18)$$

Besides, the equation of motion applied to the CSD is shown as follow,

$$m_s \ddot{x}_s + c_s \dot{x}_s + k_s x_s + F_D(\dot{x}_d, x_d) = -m_s \ddot{z}_H \quad (19)$$

where,

- m_s : first modal mass of aerogenerator
- m_d : mass of TMD
- c_s : first modal damping coefficient of aerogenerator
- c_d : damping coefficient in TMD
- k_s : first modal stiffness of aerogenerator
- k_d : stiffness element in TMD
- F_D : hysteresis damping force of CSD
- x_s : first modal displacement of aerogenerator
- x_d : displacement in TMD
- z_H : ground motion

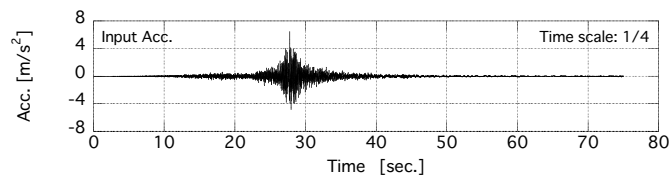
Table 3 shows the parameters for the preliminary analysis. The aerogenerator was build as a model in 1/16-scale for this study. The model size was determined by considering the experimental conditions, which is conducted in the next step of research. The analytical parameters for TMD were set at a mass ratio of 2% to that of aerogenerator, and the parameters for the CSD were similar to those for TMD with a yield displacement of 2mm. In addition, the bilinear coefficient was decided to be 1/25 which is a popular mechanical characteristic which is applicable to the general industrial structures.

Figure 8 shows the input motion used for the time history response analysis to evaluate the vibration control effect in both damping devices. The input motion is a real record measured in Kashima City during the Great East Japan Earthquake. Since the natural frequency of the target aerogenerator was 0.6Hz and that of the smaller scale model was 2.3Hz, the structural model was built in 1/4 scale. Accordingly, the time history wave and response spectrum were translated into a 1/4 scale model. Figure 9 and 10 shows the time history responses obtained from seismic analysis. The figures compare the responses of the aerogenerator in the cases of the models with non-vibration control device, with TMD, and with the CSD. Figure 11 shows the hysteresis loop of the CSD.

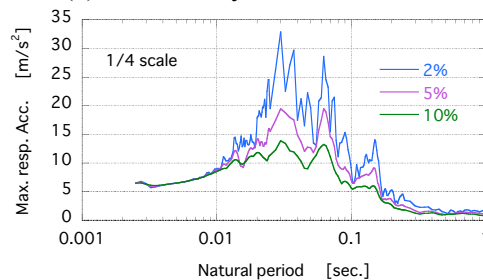
Both vibration control devices reduced the seismic responses effectively. In general, an additional mass typed device such as the TMD would be taken as more appropriate for the vibration control of the aerogenerator than the energy dissipation typed device such as the CSD because it is easier to insert the device into an aerogenerator. However, an energy dissipation typed damper has also adequate performances for the vibration control and great advantages in terms of cost. Table 4 shows the summarized results of a time history responses obtained by using root mean square averages and maximum responses. The table indicates the effectiveness of the CSD. For further study, the loading test and the shaking table test had been planned and the 1/16 scale experimental model for aerogenerator with dampers were constructed as shown in Figure12.

Table 3 Analytical parameters used for preliminary analysis

	Aerogenerator	TMD	CSD
Mass or Mass ratio	90 [kg]	2.0 [%]	1st stiffness: equivalent to 1.22 [Hz] of main structure
Damping	0.3 [%]	8.7 [%]	2nd stiffness: 1/25 of 1st stiffness
Stiffness	2.3 [Hz]	2.2 [Hz]	Yield displacement: 2.0 [mm]

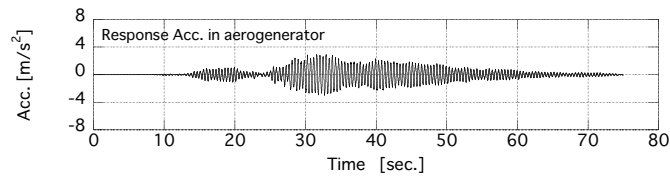


(a) Time history on acceleration

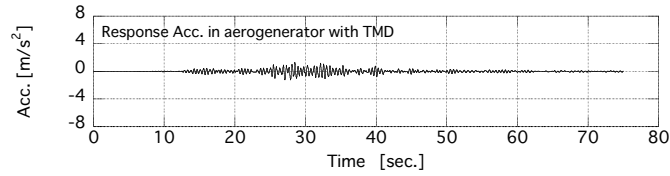


(b) Response spectrum

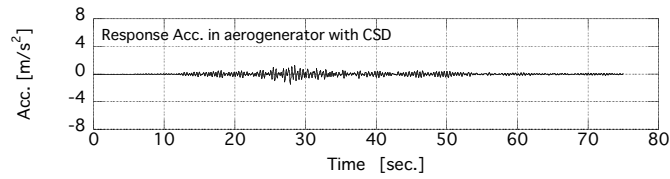
Figure 8 Input wave used in time response analysis



(a) Response acceleration in aerogenerator without vibration control device

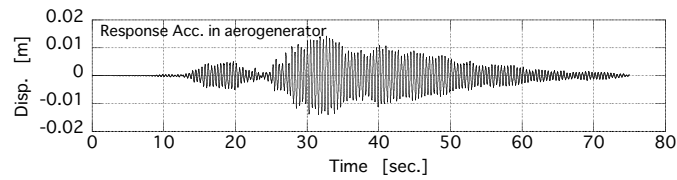


(b) Response acceleration in aerogenerator with TMD

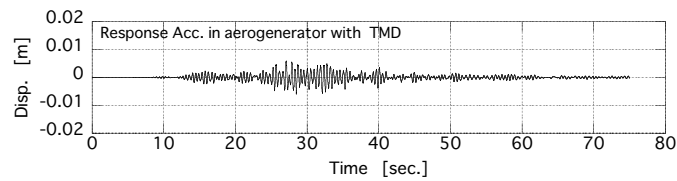


(c) Response acceleration in aerogenerator with CSD

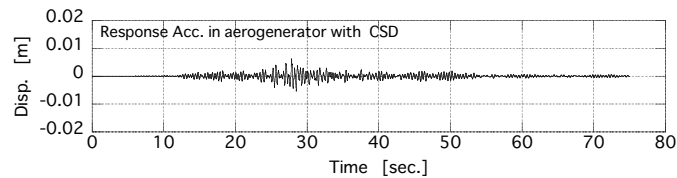
Figure 9 Time history acceleration responses of aerogenerator induced seismic motion



(a) Response displacement in aerogenerator without vibration control device

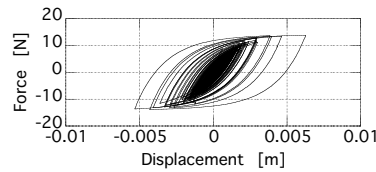


(b) Response displacement in aerogenerator with TMD



(c) Response displacement in aerogenerator with CSD

Figure 10 Time history displacement responses induced seismic motion



Hysteresis loop of CSD

Figure 11 Hysteresis loop of CSD under seismic motion

Table 4 RMS response acceleration and displacement

	Vibration control effect	
	TMD	CSD
RMS Acc. [%]	29.2	29.4
RMS Disp. [%]	26.8	22.9
Max. Acc. [%]	44.1	50.0
Max. Disp. [%]	42.1	46.0



Figure 12 1/15 scale experimental model of aerogenerator

6. Conclusions

This study has examined a response controlling effect of damper using the elasto-plastic hysteresis characteristics of a metal material applicable to an aerogenerator. The paper discusses the design method of the elasto-plastic CSD, its basic mechanical properties as evaluated from loading tests, and it presents an analytical model of the damper. Five different elasto-plastic dampers were evaluated in terms of their basic damping performance and in terms of their damping capacities with different material properties and their damping performances in small and large deformation regions. It was confirmed that the damping force and mechanical characteristics of the elasto-plastic CSD mostly meet the essential design specifications. In addition, a time history response analysis was conducted as a preliminary assessment to evaluate the response control effect using two different vibration control devices. As a result, it was confirmed that the response control effect on the acceleration and displacement responses of the CSD on the aerogenerator model was as effective as the responses with a TMD. For further study, a loading test and a shaking table test are planned using a 1/15-scale experimental model with dynamic characteristics.

ACKNOWLEDGEMENT

This work was supported by the energy technology development program of Korea Institute of Energy Technology Evaluation and Planning (KETEP) with a grant (No.20153030023760). The authors would like to express their appreciation for the financial support.

REFERENCES

- [1] Sanjay R. Arwade, Matthew A. Lackner, Mircea D. Grigoriu, 2011, “Probabilistic Models for Wind Turbine and Wind Farm Performance,” *J. Sol. Energy Eng.*, 2 133(4), pp. 041006-1-041006-9.
- [2] Ishihara, T., 2006, “Typhoon Damages and Wind Resistant Design of Wind Turbine,” “55th Japan National Congress for Theoretical and Applied Mechanics (in Japanese).
- [3] Ishihara, T., Yamaguchi, A, and Fujino, Y., 2004, “Damages of Wind Turbines Due to Typhoon 0314 and Estimation of Strong Winds : Part 1 Summary of Field Surveys,” *Journal of Japan Association for Wind Engineering*, 99, pp.69-70 (in Japanese).
- [4] T. Hassan; M. Rahman; S. Bari, 2015, “Low-Cycle Fatigue and Ratcheting Responses of Elbow Piping Components,” *J. Pressure Vessel Technol.*, 137(3), pp.031010-031010-12.
- [5] George E. Varelis; Spyros A. Karamanos; Arnold M. Gresnigt, 2012, “Pipe Elbows Under Strong Cyclic Loading,” *J. Pressure Vessel Technol.*, 135(1), pp.011207-011207-9.
- [6] Keishi Tsujita; Atsuhiko Shintani; Tomohiro Ito; Chihiro Nakagawa, 2014, “Basic Study on Vibrational Behavior of Piping Systems Supported by Elasto-Plastic Damper With Gap Support,” *Proc. ASME. 46070*, 8, Seismic Engineering, PVP2014-28283.
- [7] T. Chiba; H. Kobayashi, 1990, “Response Characteristics of Piping System Supported by Visco-Elastic and Elasto-Plastic Dampers,” *J. Pressure Vessel Technol.*, 112(1), pp.34-38.
- [8] Y. M. Parulekar, G. R. Reddy, K. K. Vaze and K. Muthumani,; Passive Control of Seismic Response of Piping Systems, *Proceedings of ASME/JSME 2004 Pressure Vessels and Piping Conference*, Seismic Engineering, Volume 2, pp.25–29, 2004
- [9] Ishigaki, H., Ishimaru, H, Hata, H. and Yoshida, A.: A Retrofit Method of a Traditional Wooden Structure by two Damper Systems, *AIJ J. of Technol. Des.*, pp. 91-96 (in Japanese).
- [10] Fukasawa, T., Fujita, S., Kurabayashi, H. and Kinoshita, A.: Study of Earthquake Isolation System Using Vertically Utilized Coiled Springs : 1st Report, Static Tests for Elastic Coiled Spring(Mechanical Systems), *J. of Japan Society of Mech. Eng.*, Vol.C , 74(739), 2008, pp. 506-512 (in Japanese).
- [11] M. A. Bhatti and K. S. Pister,; A Dual Criteria Approach for Optimal-Design of Earthquake-Resistant Structural Systems, *Earthquake Engineering & Structural Dynamics*, 9(6), 1981, pp. 557-572..